4 **Беспалов, Ю. А.** Многокомпонентные системы на основе полимеров / Ю. А. Беспалов, Н. Г. Коновалов. – Л.: Химия, 1981. – 88 с.

5 **Blends of polycarbonate and polysulphone-polydimethyl-siloxane block copolymers: analysis of compatibility and impact strength** / S. S. Pesetskii [etc.] // Journal of Applied Polymer Science. – 1999. – Vol. 73. – P. 1823–1834.

6 **Influence of Interfacial Agents on the Physicochemical Characteristics of Binary Polyethylene/Polyamide 6 and Ternary Polyethylene/Polypropilene/Polyamide 6 Blends** / P. L. Beltrame [etc.] // Journal of Applied Polymer Science. – 1996. – Vol. 60. – № 4. – P. 579–590.

7 **Samios, C. K.** Compatibilization of poly(ethylene terephtalate) / C. K. Samios, N. K. Kalfoglou / Polyamide-6 alloys: Mechanical, thermal and morphological characterization // Polymer. – 1999. – Vol. 40. – № 17. – P. 4811–4819.

8 **Измерение аттракционного взаимодействия технических поверхностей** / А. Я. Григорьев [и др.] // Трение и износ. – 2003 (24). – № 4. – С. 405 – 412.

S. P. BOGDANOVICH, I. N. KOVALIOVA

ROLE OF COMPATIBILIZER CONCENTRATION AND COMPOSITION IN PA6/PE POLYMER MIXTURE FRICTION AND WEAR

The effect of high-density polyethylene compatibilizing additives on mechanical and tribological properties of polyamide 6/high-density polyethylene mixture was studied. The percentage of compatibilizers (C) in the general polyolefin content was from 0 to 100 %. In addition, the chemical composition of C was changed by grafting different amounts of carboxyl groups to macromolecules of polyethylene. The range of optimal concentrations of C – from 25 to 75 % of the total polyolefin component – allowing to obtain the best combination of mechanical and tribological characteristics of polyamide 6/polyethylene mixture was identified.

Получено 28.12.2010

ISBN 978-985-468-924-1. Mechanics. Scientific researches and methodical development. Vol. 5. Gomel, 2011

UDC 666.653

P. VERA SERNA
Universidad Politécnica de Tecámac, Tecámac, Mexico
A. M. BOLARIN MIRO, F. SANCHEZ DE JESUS
Universidad Autónoma del Estado de Hidalgo, Mineral de la Reforma, Mexico

CHARACTERIZATION OF MANGANESE FERRITES OBTAINED BY MECHANOSYNTHESIS

Manganese ferrite $MnFe_2O_4$ was obtained by mechanosynthesis, high energy milling was used and chemical reaction was based on precursor oxides Fe_2O_3 and MnO. Charac-

terization showed magnetic saturation of 49,77 emu/g, and when the milling time was 16 hours the magnetic saturation decreased due to increment of volume in phases FeO and Fe, irregular morphology was observed, spinel structure at 12 hours of milling with the maximum value of spinel phase was found, the results of Raman technique showed the change in octahedral and tetrahedral sites.

Introduction. Ferrites are ceramics studied since 1909 with applications in storage data devices, heart valves, microwave devices, MRI contrast, telecommunication parts and pigments, etc. [1–4]. The magnetic and electric properties of ferrites depend on such factors as crystalline structure and particle size, the process of mechanosynthesis has the characteristic to promote nanometric sizes. Sometimes the variations in some factors get different saturation magnetic values [5, 6].

There are different methods in ceramic synthesis such as coprecipitation, sol-gel, calcination, hydrothermal and mechanosynthesis [1, 7, 8]; some methods need variations in the temperature, pH control or the use of acids to get the chemical reaction, it causes such problems as high demand of electric energy, consumption of combustible fuel and contamination with acids. A method at ambient temperature and without use of acid is the mechanosynthesis method, it consists of getting chemical reaction by adding mechanic energy [9].

Ferrite $MnFe_2O_4$ is a soft magnetic material with spinel structure, its structure has two octahedral and one tetrahedral sites, spinel structure facilitates the increase of value of magnetic saturation [10].

The work shows the synthesis of manganese ferrite $MnFe_2O_4$ from MnO and Fe_2O_3 and results of magnetic saturation, morphology, crystalline phases and Raman characterization.

Experimental Procedure. Powder oxides MnO and Fe_2O_3 from Sigma-Aldrich with purity 99 % were used in milling process, milling times from 0 to 16 hours, the equipment utilized was a SPEX 8000D Mixer/Mill, with stainless steel vial (50 cm^3) and six steel balls (12,7 mm diameter), volume ratio 1:8, at room temperature under air atmosphere.

Reaction

$$MnO+Fe_2O_3 \longrightarrow MnFe_2O_4.$$

Powders were characterized by X-ray diffraction (XRD) using a Philips P1710 diffractometer with CoKα (l = 0,17902 nm) radiation. Patterns were collected in 2θ interval of 20–90° with increments of 0,05 (2θ). The Rietveld refinement was used to determine volume of phases and crystal size, MAUD was the software utilized. Magnetic saturation was measured at room temperature, using vibrating sample magnetometer, fields applied were between –12000 and 12000 Oesterds. Powder morphology was observed with a scanning electron microscope using a JEOL 6300, with 20 kV. Raman characterization was with a spectrometer Spectrum GX Perkin Elmer, NIR FT-Raman. The observation range was 300 to 800 cm^{-1}.

Results and discussion. At different milling times between 0 and 12 hours, the best result of synthesis was obtained at 12 hours of milling. The figure 1 shows the XRD spectrums with results correspond to 12 and 16 hours of milling. In the case of spectrum for 12 hours the peaks corresponding to ferrite $MnFe_2O_4$ at 20,9°, 34,6°, 40,8°, 49,7°, 62°, 66,3°, 73,2°, 87,3° were observed. The results show there are few percents of iron phase detected on 52,4° and low intensity in peaks of iron oxide II (FeO) at 42º, 48,9º and 71,6º. The synthesis was possible because the precursors oxides had cubic structure like it was established by Hume Rothery rules, the powder ratio was adequate to chemical reaction and the energy added by mechanosynthesis was sufficient. The diffraction results show at 16 hours of milling the FeO and Fe phases increase due to possible contamination of vials and balls.

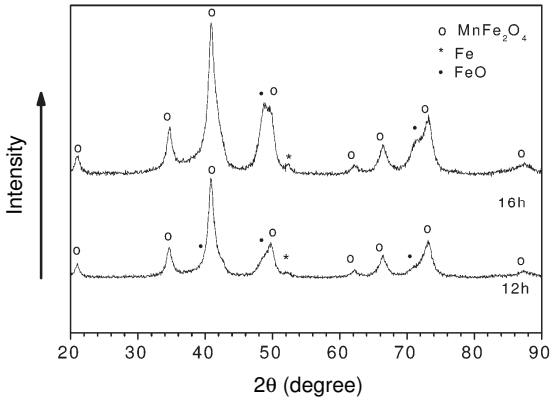

Figure 1 – The XRD patterns for the studied products at 12 and 16 hours of milling

Table 1

Composition	Phases	% Volume Phase	Red Parameter
A	$MnFe_2O_4$	93,31	a = 8,499
	MnO	0,01	a = 4,284
	FeO	6,67982	a = 4,356

The results of spectroscopy Raman (figure 2) show the changes in tetrahedral and octahedral sites at the different milling time. Between 9 and 12 hours it is possible to see the change on the peaks upon 650 cm^{-1}. The characterization presented by Yu [11] shows the Raman spectrum of a spinel structure, determining that the crests in lines after 600 cm^{-1} corresponding to tetrahedral sites while the peaks that occur at lower values 600 cm^{-1} correspond to octahedral sites. At a time of 0 hours, there is no spinel structure, in the line of 1 hour the process distinguishes the presence of the first sites of iron, after 3 hours octahedral sites are changed due to the movement of cations, at 9 hours of milling the spinel structure are observed,

finally after 12 hours for both tetrahedral iron sites, presenting a broad peak at 660 are observed while octahedral sites for the iron and manganese in 400 and 500 are observed. In that curve the amplitude of the peak has been increased with respect to the results at 9 hours, the increase in width of peak in the line at 12 hours, indicating that the material is more susceptible to magnetization. As shown in figure 2 the intensity increase at 12 hours gives the possibility to distinguish the reduction of line distortions showing a response curves in the sites of the spinel. Thus the effect can be seen at synthesis by mechanochemical method that leads to an adequate diffusion for the formation of spinel structure oxides from precursors of cubic structure.

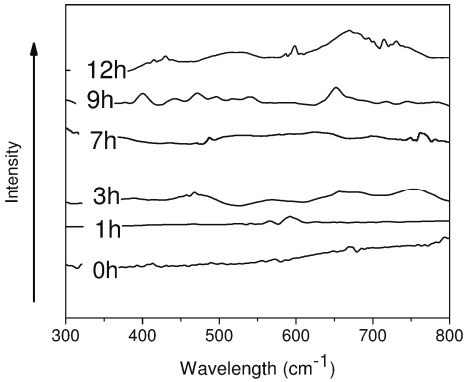

Figure 2 – Results of Raman spectroscopy at milling times 0 to 12 h

Figure 3 shows the images corresponding to different milling times where can be seen that the particles have irregular morphology, featuring some agglomerates caused by the milling process and the particles are of sizes between 0,4 and 0,6 micrometers.

In micrograph 3, *a* there is observed the homogeneity on the particle size of powder before starting the milling process. Figure 3, *b* shows particles and agglomerates of various sizes and the increase in size due to deformation and welding, while micrograph 3, *c* shows that it is possible to observe particles and agglomerates larger than in micrograph 3, *b.* After 9 hours in figure 3, *d* there are minor variations in size with respect to the milling time, these smaller sizes are beneficial for synthesis because there is a greater surface area to promote the reaction, in figure 3, *e* with 12 hours of milling particles are observed between 400 and 500 nm, the energy input has been achieved at synthesis. In figure 3, *f* size particles with fewer agglomerates are observed.

The process generated by mechanosynthesis can be observed in particle and agglomerate size variations. First there are agglomerated particles. The formation of agglomerates is observed during a time of three hours, their average size de-

creases with the increasing grinding time reaching the proper size at the time of 9 to 12 hours.

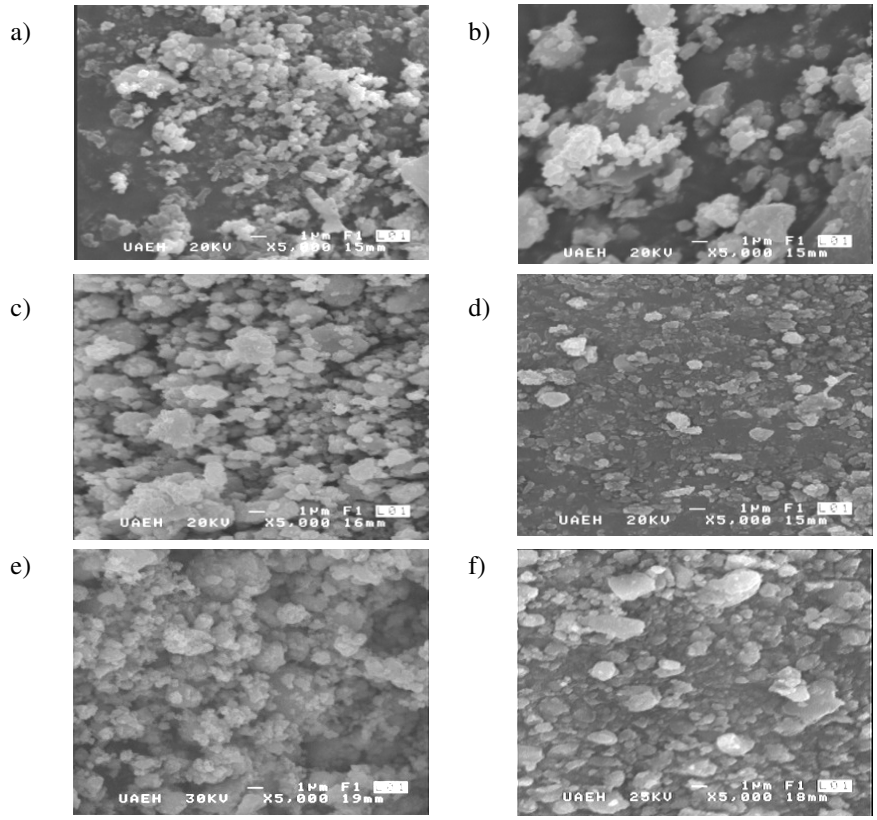

Figure 3 – Micrographs at different times: a – 0 h; b – 3 h; c – 7 h; d – 9 h; e – 12 h; f – 16 h

Average size of a particle. The change of particle size in the process of mechanosyntesis usually begins with the grow of a particle due to the deformation of particles or welded particles as shown in figure 4. The increase of average size results in promoting the diffusion of atoms, with particle growth the accumulation of the stress and deformation increases. When the particles achieve big size the fractures promoting the formation of new surfaces to facilitate the synthesis reaction occur. As it can be seen in the Raman results between one and seven hours lines, the spinel curve reported by Yu isn't detected. It happens in concordance with the new surfaces generated after 9 hours when the particle size is reduced and at 12 hours the last one in accordance with the high value in volume percentage of

manganese is detected with XRD, keeping the proper size of new compound. The results at 12 hours in particle sizes between 80 nm and 6 micrometers in the composition are detected.

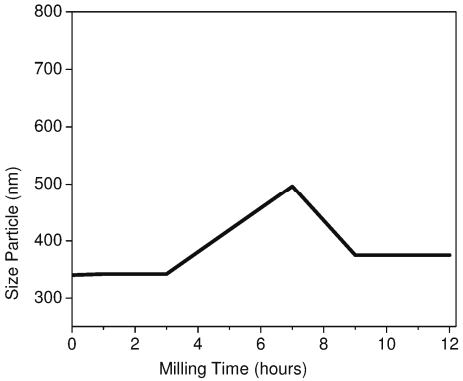

Figure 4 – Distribution of average size of the particle at 0 h, 3 h, 7 h, 9 h and 12 h

Previous characterizations provide information about the results to be presented in this section due to the formation of spinel structure detected by XRD. The highest proportion is to 12 hours of milling, the increase in amplitude of the peaks width is observed in tetrahedral and octahedral sites in Raman analysis. The particle size the contamination to 16 hours of milling decreases the value of magnetic saturation. All factors modify the magnetic results at every time of milling as shown in figure 5.

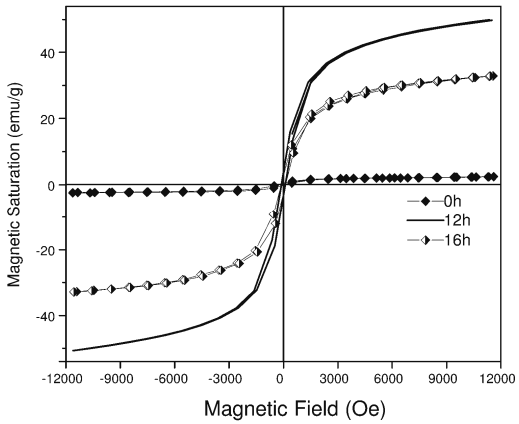

Figure 5 – Curves of magnetic saturation with milling time 0 h, 12 h, and 16 h

REFERENCES

1 **Sugimoto, M.** The past, present and future of ferrites / M. Sugimoto // Journal of American Ceramics Society. – 1999. – Vol. 82. – № 2. – P. 269–280.

2 **Chondros, T. G.** Fatigue fracture of the Björk-Shiley heart valve strut and failure diagnosis from acoustic signatures / T. G. Chondros // Theoretical and Applied Fracture Mechanics. – 2010. – Vol. 54. – № 2. – P. 71–81.

3 **Ahmed, N. M.** Tailored ferrites-kaolin anticorrosive hybrid pigments in solvent-based paints for protection of cold-rolled steel / N. M. Ahmed, M. M. Selim / Pigment and Resin Technology. – 2010. – Vol. 39. – № 2. – P. 101–111.

4 **Water-Soluble Spinel Ferrites by a Modified Polyol Process as Contrast Agents in MRI** / G. Basina [etc.] // AIP Conference Proceedings. – 2010. – Vol. 1311. – № 1. – P. 441–446.

5 **The preparation of magnetic nanoparticles for applications in biomedicine** / P. Tartaj [etc.] // Journal of Physics D: Applied Physics. – 2003. – Vol. 36. – P. 182–197.

6 **Tuning the Thermal Stability of Molecular Precursors for the Nonhydrolytic Synthesis of Magnetic $MnFe_2O_4$ Spinel Nanocrystals** / Q. Song [etc.] // Chemistry of Materials. – 2007. – Vol. 19. – № 19. – P. 4633–4638.

7 **Zahi, S.** Synthesis, Permeability and Microstructure of the Optimal Nickel-Zinc Ferrites by Sol-Gel Route / S. Zahi // Journal of Electromagnetic Analysis and Applications. – 2010. – Vol. 2. – № 1. – P. 56–62.

8 **Two alternative synthesis routes for MnZn ferrites using mechanochemical treatments** / P. M. Botta [etc.] // Ceramics International. – 2006. – Vol. 32. – № 8. – P. 857–863.

9 **Botta, P. M.** Kinetic study of $ZnFe_2O_4$ formation from mechanochemically activated $Zn–Fe_2O_3$ mixtures / P. M. Botta, E. F. Aglietti, J. M. Porto López // Materials Research Bulletin. – 2006. – Vol. 41. – № 4. – P. 714–723.

10 **Vestal, C. R.** Synthesis and Magnetic Characterization of Mn and Co Spinel Ferrite-Silica Nanoparticles with Tunable Magnetic Core / C. R. Vestal, Z. J. Zhang // Nano Letters. – 2003. – Vol. 3. – № 12. – P. 1739–1743.

11 **Cation migration and magnetic ordering in spinel $CoFe_2O_4$ powder: micro-Raman scattering study** / T. Yu [etc.] // Journal of Physics: Condensed Matter. – 2002. – Vol. 14. – № 37. – P. L613–L618.

П. ВЕРА СЕРНА, А. М. БОЛАРИН МИРО, Ф. САНЧЕС ДЕ ХЕСУС

ХАРАКТЕРИСТИКИ ФЕРРИТА МАРГАНЦА, ПОЛУЧЕННОГО МЕХАНОСИНТЕЗОМ

Феррит марганца $MnFe_2O_4$ был получен механосинтезом с использованием высокой энергии размалывания и химической реакции на базе первичных оксидов Fe_2O_3 и MnO. Установлено, что насыщение при намагничивании составляет 49,77 $А·м^2/кг$. При времени помола 16 часов магнитное насыщение снижается из-за приращения объема фаз FeO и Fe, наблюдается нерегулярная морфология. Было обнаружено, что при 12-часовом помоле величина фазы шпинели максимальна. Результаты Рамановского исследования выявили изменение расположения октаэдрических и тетраэдрических узлов.

Получено 01.02.2011